Yttrium and Lanthanide Complexes with Various P,N Ligands in the Coordination Sphere: Synthesis, Structure, and Polymerization Studies

Michael T. Gamer,[a] Marcus Rastätter,[a] Peter W. Roesky,*[a] Alexandra Steffens,[b] and Mario Glanz*[c]

In memoriam Professor Oskar Glemser

Abstract: Yttrium and lanthanide complexes with different P,N ligands in the coordination sphere have been synthesized. First the chloride complexes $[\{CH(PPh_2NSiMe_3)_2\}Ln\{(Ph_2P)_2N\}Cl]$ (Ln = Y (**1a**), La (**1b**), Nd (**1c**), Yb (**1d**)) having the bulky $[CH(PPh_2NSiMe_3)_2]^-$ and the flexible $[(Ph_2P)_2N]^-$ ligands in the same molecule were prepared by three different synthetic pathways. Compounds **1a–d** can be obtained by reaction of $[\{[CH(PPh_2NSiMe_3)_2]LnCl_2\}_2]$ with $[K(thf)_nN(PPh_2)_2]$ ($n = 1.25$, 1.5) or by treatment of $[\{(Ph_2P)_2N\}LnCl_2(thf)_3]$ with $K[CH(PPh_2NSiMe_3)_2]$. Furthermore, a one-pot reaction of $K[CH(PPh_2NSiMe_3)_2]$ with $LnCl_3$ and $[K(thf)_nN(PPh_2)_2]$ leads to the same products. Single-crystal X-ray structures of **1a–d** show that the conformation of the six-membered metallacycle (N1-P1-C1-P2-N2-Ln) which is formed by chelation of the $[CH(PPh_2NSiMe_3)_2]^-$ ligand to the lanthanide atom is influenced by the ionic radius of the central metal atom. In solution dynamic behavior of the $[(Ph_2P)_2N]^-$ ligand is observed, which is caused by rapid exchange of the two different phosphorus atoms. Further reaction of **1b** with $KNPh_2$ resulted in $[\{(Me_3SiNPPh_2)_2CH\}La\{N(PPh_2)_2\}(NPh_2)]$ (**2**). Compounds **1a–d** and **2** are active in the ring-opening polymerization of ε-caprolactone and the polymerization of methyl methacrylate. In some cases high molecular weight polymers with good conversions and narrow polydispersities were obtained. In both polymerizations the catalytic activity depends on the ionic radius of the metal center.

Keywords: chelates · lanthanides · N,P ligands · polymerization · yttrium

Introduction

Since the early 1990s, metallocenes of the lanthanides have been well established as catalysts for the polymerization of polar monomers such as acrylates, lactones, lactides, isocyanates, and oxiranes.[1] Thus, for the polymerization of methyl methacrylate Yasuda et al. used the catalyst $[\{(\eta^5\text{-}C_5Me_5)_2SmH\}_2]$ and established the mechanism of this catalytic process. Monodisperse, high molecular weight polymers with extremely narrow polydispersities were obtained.[2] In the established mechanism, the carbonyl group of the monomer is activated by coordination to the Lewis acidic lanthanide center. A comparable bimetallic mechanism was established for the polymerization of ε-caprolactone and methyl methacrylate starting from the divalent lanthanide precatalyst $[(\eta^5\text{-}C_5Me_5)_2Sm(thf)_2]$.[3] Today this mechanism has also been established for other monomers and other metallocenes of the lanthanides.[4] For the cyclic esters ε-caprolactone and δ-valerolactone, a diversity of lanthanide catalysts, such as metallocenes[5] and alkoxide complexes, were established.[6] The role of the ancillary ligand set, which remains bound to the metal center during the whole process, is to limit the number of active polymerization sites on the metal atom and to modify the reactivity of the metal throughout the polymerization.[5d]

Recently, in lanthanide chemistry there have been significant research efforts to establish amides as ancillary ligands. One approach is the use of P,N compounds such as phosphinimides (R_2PNR'),[7] phosphoraneiminato (R_3PN),[8] phos-

[a] Dr. M. T. Gamer, Dipl.-Chem. M. Rastätter, Prof. Dr. P. W. Roesky
Institut für Chemie, Freie Universität Berlin
Fabeckstrasse 34–36, 14195 Berlin (Germany)
Fax: (+49) 30-838-52440
E-mail: roesky@chemie.fu-berlin.de

[b] Dipl.-Chem. A. Steffens
Institut für Chemie, Sekr. C2, Technischen Universität Berlin
Strasse des 17. Juni 135, 10623 Berlin (Germany)

[c] Dr. M. Glanz
Fachgruppe I.3 der Bundesanstalt für Materialforschung und -prüfung
12200 Berlin (Germany)

 DOI: 10.1002/chem.200401062

phiniminomethanides ($(RNPR'_2)CH$),[9,10] phosphiniminomethanediides ($(RNPR'_2)C$),[11] and diiminophosphinates ($(R_2P(NR'))$[12] as ligands. Current work on these ligands has shown that some lanthanides complexes having P,N ligands in the coordination sphere[8] may not only exhibit unusual coordination modes, but also can be used as catalysts for ε-caprolactone polymerization.[13] Lately, the homoleptic diphosphinoamide complexes $[Ln\{N(PPh_2)_2\}_3]$ (Ln = Y, La, Nd, Er) were synthesized by us.[14] The complexes show η^2 coordination of the $[(Ph_2P)_2N]^-$ ligand in the solid state and dynamic behavior in solution. $[Ln\{N(PPh_2)_2\}_3]$ was also used as an efficient catalyst for the polymerization of ε-caprolactone.[14]

Currently, we are investigating the reactions of lanthanides with the very bulky bis(phosphinimino)methanide ligand $[CH(PPh_2NSiMe_3)_2]^-$. We previously reported the synthesis of a series of yttrium and lanthanide bis(phosphinimino)methanide dichloride complexes $[\{[CH(PPh_2NSiMe_3)_2]LnCl_2\}_2]$ (Ln = Y, Sm, Dy, Er, Yb, Lu)[9] by reaction of $K[CH(PPh_2NSiMe_3)_2]$[15] with the corresponding metal trichlorides. Furthermore, we reported reactions of $[\{[CH(PPh_2NSiMe_3)_2]LnCl_2\}_2]$ leading to the corresponding amido complexes $[\{CH(PPh_2NSiMe_3)_2\}Ln(NPh_2)_2]$ (Ln = Y, Sm),[9] cyclopentadienyl complexes, $[\{CH(PPh_2NSiMe_3)_2\}Ln(\eta^5\text{-}C_5H_5)_2]$ (Ln = Y, Sm, Er),[10] and cyclooctatetraene bis(phosphinimino)methanide complexes $[\{CH(PPh_2NSiMe_3)_2\}Ln(\eta^8\text{-}C_8H_8)]$ (Ln = Y, Sm, Er, Yb, Lu).[16]. The latter can act as catalysts for the hydroamination/cyclization reaction. The very bulky $[CH(PPh_2NSiMe_3)_2]^-$ ligand can be used to direct the substitution pattern on the lanthanide atom just by the steric demand of the ancillary ligands.

Here we report on the combination of the bulky $[CH(PPh_2NSiMe_3)_2]^-$ ligand and the flexible $[(Ph_2P)_2N]^-$ ligand in one complex. In addition to the syntheses and solid-state structures of the complexes obtained, we were interested in studying the influence of both P,N systems as spectator ligands in the polymerization of polar monomers.

Results and Discussion

Chloro complexes: The chloro complexes $[\{CH(PPh_2NSiMe_3)_2\}Ln\{(Ph_2P)_2N\}Cl]$ (Ln = Y (**1a**), La (**1b**), Nd (**1c**), Yb (**1d**)) can be obtained by three different synthetic approaches. All synthetic approaches were established for the yttrium complex **1a**, whereas the other complexes were obtained only by one or two approaches (Scheme 1).[17] The first approach starts from the well-established lanthanide dichloride compound $[\{[CH(PPh_2NSiMe_3)_2]LnCl_2\}_2]$,

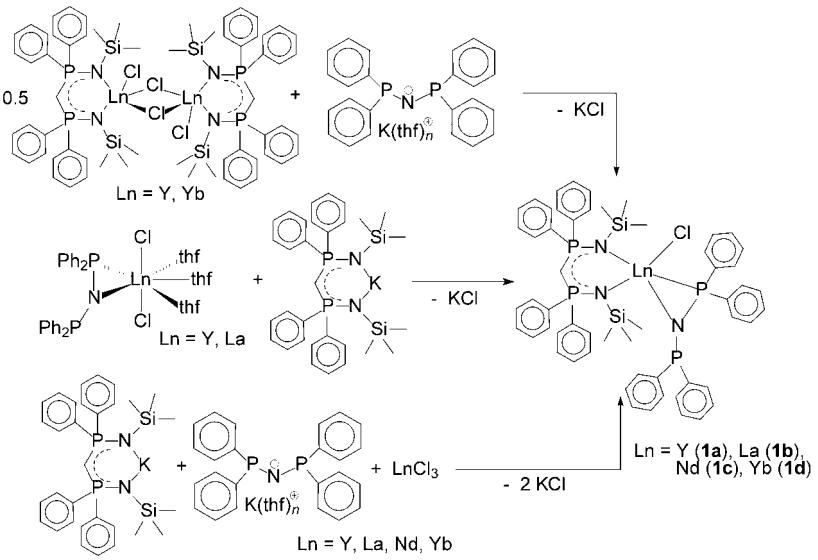

Scheme 1. Synthesis of **1a**–**d**.

which was treated with $[K(thf)_nN(PPh_2)_2]$ ($n = 1.25$, 1.5) in a 1:2 molar ratio in THF to afford the corresponding bis(phosphinimino)methanide complexes (Scheme 1).[17] This route does not yield **1b**, as the bis(phosphinimino)methanide lanthanide dichloride complexes could not be obtained for metal centers larger than samarium. Compound **1** is also accessible by reaction of $[\{(Ph_2P)_2N\}LnCl_2(thf)_3]$[18] with $K[CH(PPh_2NSiMe_3)_2]$ in a 1:1.1 molar ratio in THF at room temperature (Scheme 1). However, the most convenient approach to **1a**–**d** is a one-pot reaction in which the potassium methanide $K[CH(PPh_2NSiMe_3)_2]$ is treated with anhydrous yttrium or lanthanide trichlorides and $[K(thf)_nN(PPh_2)_2]$ in a 1:1:1 molar ratio in THF (Scheme 1). The new complexes were characterized by standard analytical/spectroscopic techniques, and the solid-state structures of all four compounds were established by single-crystal X-ray diffraction (Figure 1).

The influence of the ionic radius of the lanthanides can be seen in the single-crystal X-ray structures. Compounds with lanthanides having a smaller ionic radius (**1a** and **1d**) are isostructural and crystallize in the triclinic space group $P\bar{1}$. Compound **1b** crystallizes in the monoclinic space group $P2_1/c$ and has four molecules of **1b** and four molecules of THF in the unit cell. Compound **1c** crystallizes in the triclinic space group $P\bar{1}$ with one toluene molecule in the unit cell. The influence of the central metal atom is not only seen in the different metrics of the unit cell but also in the geometry of the molecule. Particularly the conformation of the six-membered metallacycle (N1-P1-C1-P2-N2-Ln) which is formed by chelation of two trimethlysilylimine groups to the lanthanide atom is influenced by the ionic radius of the cen-

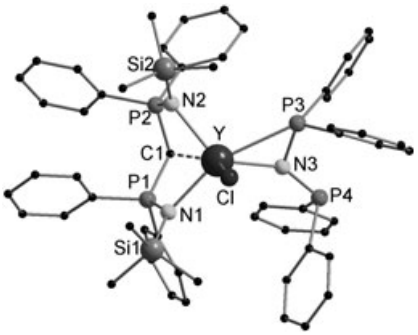

Figure 1. Solid-state structure of **1a** showing the atom labeling scheme and omitting hydrogen atoms. Selected bond lengths [pm] and angles [°] (also given for isostructural **1b**–**1d**): **1a**: Y–C1 265.5(4), Y–N1 232.2(4), Y–N2 238.5(3), Y–N3 231.6(4), Y–P3 287.8(2), Y–Cl 256.6(2), P1–C1 174.7(4), P2–C1 175.1(4), N1–P1 160.7(3), N2–P2 160.6(3), N3–P3 168.6(3), N3–P4 171.4(3); N3-Y-N1 121.67(12), N3-Y-N2 129.24(12), N1-Y-N2 97.68(12), N3-Y-Cl 103.07(9), N1-Y-Cl 92.25(10), N2-Y-Cl 106.22(10), N3-Y-C1 102.27(12), Cl-Y-C1 152.74(9). **1b**: La–C1 280.2(4), La–N1 250.2(4), La–N2 249.7(3), La–N3 244.8(3), La–P3 305.33(12), La–Cl 274.40(13), P1–C1 173.1(4), P2–C1 172.2(4), N1–P1 160.2(4), N2–P2 159.9(4), N3–P3 167.3(4), N3–P4 171.8(4); N3-La–N1 110.15(11), N3-La–N2 114.66(12), N1-La–N2 117.32(11), N3-La-Cl 127.05(9), N1-La-Cl 92.59(9), N2-La-Cl 93.39(10), N3-La-C1 118.79(12), Cl-La-C1 114.07(9). **1c**: Nd–C1 285.0(4), Nd–N1 247.8(3), Nd–N2 243.3(3), Nd–N3 234.3(3), Nd–P3 287.54(11), Nd–Cl 265.67(11), P1–C1 173.0(4), P2–C1 174.6(4), N1–P1 159.1(3), N2–P2 159.6(3), N3–P3 166.8(3), N3–P4 171.4(3); N3-Nd-N1 116.04(11), N3-Nd-N2 128.48(11), N1-Nd-N2 93.72(11), N3-Nd-Cl 97.00(8), N1-Nd-Cl 127.22(8), N2-Nd-Cl 96.21(8), N3-Nd-C1 96.04(11), Cl-Nd-C1 158.28(8). **1d**: Yb–C1 262.7(4), Yb–N1 229.1(4), Yb–N2 235.8(4), Yb–N3 226.8(4), Yb–P3 284.0(2), Yb–Cl 252.6(2), P1–C1 175.8(4), P2–C1 175.8(4), N1–P1 161.0(4), N2–P2 159.8(4), N3–P3 169.6(4), N3–P4 172.1(4); N3-Yb-N1 121.35(13), N3-Yb-N2 129.77(13), N1-Yb-N2 98.42(13), N3-Yb-Cl 102.91(11), N1-Yb-Cl 92.07(11), N2-Yb-Cl 105.08(11), N3-Yb-C1 101.81(14), Cl-Yb-C1 153.57(10).

tral metal atom. The ring adopts a twist-boat conformation in which the central carbon atom and the lanthanide atom are displaced from the N_2P_2 least-squares plane. The displacement depends on the metal center and on the packing in the solid state. Whereas in compound **1b** the La atom is displaced only by 23.3 pm and thus is almost within the N_2P_2 least-squares plane, in **1d** the ytterbium atom is 136.2 pm out of plane. In contrast the methine carbon atoms (C1) are displaced in both cases out of the plane (61.7 pm in **1b** and 78.4 pm in **1d**; Figure 2). The difference in metallacycle geometry of **1b** compared to **1a**, **1c**, and **1d** is also seen in the P1-C1-P2 angle, which is significantly larger in **1b** (138.1(2)°) than in the other compounds (123.8(2)° (**1a**), 127.7(2)° (**1c**), 122.8(2)° (**1d**)). The Ln–C1 distances (262.7(4) (**1b**) to 280.2(4) pm (**1d**)) are longer than usual.[9,10,16,19] However, the folding of the six-membered ring towards the lanthanide atom is caused by a weak interaction. The Ln–C1 bond lengths increase with increasing ionic radius of the metal center. The resultant tridentate coordination of the ligand was observed earlier.[9,10,16,20] The Ln–N bond length strongly depends on the location of the $[(Ph_2P)_2N]^-$ ligand in the molecule. In **1b**, the $[(Ph_2P)_2N]^-$ ligand is almost symmetrically located between N1 and N2, and the La–N1 (250.2(4) pm) and La–N2 (249.7(3) pm) bond lengths are almost identical. In contrast, in **1a**, **1c**, and **1d** the $[(Ph_2P)_2N]^-$ ligand is twisted out of its symmetrical position. As a result of the steric repulsion of the phenyl rings in both ligands, the Ln–N1 (232.2(4) (**1a**), 247.8(3) (**1c**), 229.1(4) pm (**1d**)) and Ln–N2 distances (238.5(3) (**1a**), 243.3(3) (**1c**), 235.8(4) pm (**1d**)) differ. The geometry within the $[CH(PPh_2NSiMe_3)_2]^-$ ligand is as expected. The P–N and P–C bond lengths vary only slightly in the series **1a**–**d**.

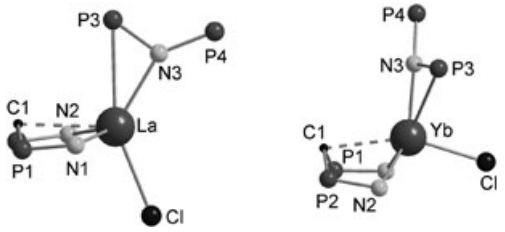

Figure 2. Solid-state structures of **1b** (left) and **1d** (right) showing the atom labeling scheme and omitting the phenyl rings, the Me_3Si groups, and the hydrogen atoms. The different conformations of the six-membered metallacycle (N1-P1-C1-P2-N2-Ln) depend on the ionic radius of the central metal atom and the packing in the solid state.

As observed in the mono-substituted diphosphanylamide complexes $[\{(Ph_2P)_2N\}LnCl_2(thf)_3]$ the diphosphanylamide ligands in **1a**–**d** are η^2-coordinated through the nitrogen atom and one phosphorus atom. Thus, one of the phosphorus atoms of the ligand binds to the lanthanide center, and the other phosphorus atom is bent away. The Ln–N3 and Ln–P3 bond lengths are 231.6(4) and 287.8(2) pm (**1a**), 244.8(3) and 305.33(12) pm (**1b**), 234.3(3) and 287.54(11) pm (**1c**), and 226.8(4) and 284.0(2) pm (**1d**), respectively. The electron lone pair of the nonbonded phosphorus atom points away from the lanthanide center. In the ligand the P–N bond length varies slightly. The phosphorus atom which binds to the lanthanide atom is located slightly closer to the nitrogen atom (N3–P3 168.6(3) (**1a**), 167.3(4) (**1b**), 166.8(3) (**1c**), 169.6(4) pm (**1d**); N3–P4 171.4(3) (**1a**), 171.8(4) (**1b**), 171.4(3) (**1c**), 172.1(4) pm (**1d**)).

The NMR spectra of diamagnetic compounds **1a** and **1b** were investigated. They are in agreement with the solid-state structures. The ^1H NMR spectra of **1a** and **1b** show characteristic sharp singlets for the Me_3Si groups and triplets for the methine protons. The methine signal of **1a** ($\delta =$ 1.63 ppm) shows an upfield shift compared to $[\{[CH(PPh_2NSiMe_3)_2]YCl_2\}_2]$ ($\delta = 1.93$ ppm). In both **1a** and **1b** the signals of the methine protons are broadened. The phenyl region in the ^1H NMR spectra is as expected. More characteristic are the $^{31}P\{^1H\}$ NMR spectra. Complexes **1a** and **1b** each show two sharp signals in the $^{31}P\{^1H\}$ NMR spectrum ($\delta = 20.6$, 41.2 (**1a**); 19.3, 41.3 ppm (**1b**)), that is, the phosphorus atoms of each ligand are chemically equivalent in solution at room temperature. Dynamic behavior of the $[(Ph_2P)_2N]^-$ ligand was also observed in all other lanthanide complexes reported so far.[14,18,21] In the $^{31}P\{^1H\}$ NMR spectrum of the yttrium complex **1a** a $^2J(P,Y)$ coupling of 7.7 Hz is observed for both signals.

Diphenylamido complexes: To learn more about the reactivity of complexes **1a–d** and especially to have a different leaving group than chloride in the catalytic reactions, we were interested in synthesizing a amido derivatives of **1a–d**. Reaction of $KNPh_2$ with **1b** in a 1:1 molar ratio in toluene at room temperature afforded the corresponding diphenylamido complex $[\{(Me_3SiNPPh_2)_2CH\}La\{N(PPh_2)_2\}(NPh_2)]$ (**2**) (Scheme 2).[17] The complex was characterized by ^1H, $^{13}C\{^1H\}$, ^{29}Si, and $^{31}P\{^1H\}$ NMR spectroscopy and elemental analysis. In the ^1H NMR spectrum of **2**, the phenyl region is very crowded. More characteristic is the signal of the methine proton of the $[CH(PPh_2NSiMe_3)_2]^-$ ligand, which in the ^1H NMR and the $^{13}C\{^1H\}$ NMR spectra is well resolved into a triplet (^1H: $\delta = 1.94$ ppm, $^3J(H,P) = 5.1$ Hz; $^{13}C\{^1H\}$: $\delta = 16.3$ ppm, $^2J(C,P) = 110$ Hz). The remaining signals are not significantly shifted compared to the starting material **1b**. In the $^{31}P\{^1H\}$ NMR spectrum of **2** the expected two peaks ($\delta = 19.9$, 43.1 ppm) of the $[CH(PPh_2NSiMe_3)_2]^-$ and $[(Ph_2P)_2N]^-$ ligands are observed.

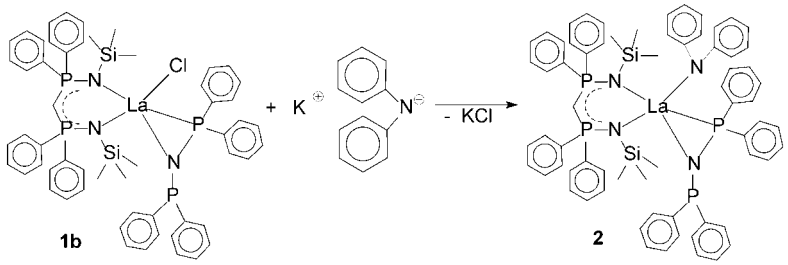

Scheme 2. Synthesis of **2**.

The solid-state structure of **2** was established by single crystal X-ray diffraction (Figure 3). Compound **2** crystallizes in the monoclinic space group $P2_1/n$ with four molecules in the unit cell. It can be clearly seen that the $[NPh_2]^-$ ligand fits well into the remaining pocket between the $[CH(PPh_2NSiMe_3)_2]^-$ and $[(Ph_2P)_2N]^-$ moieties. As observed for **1a–d**, a six-membered ring (N1-P1-C1-P2-N2-La) which adopts a twist-boat conformation is formed by the $[CH(PPh_2NSiMe_3)_2]^-$ ligand and the lanthanum atom. The lanthanum atom in **2** shows a significantly larger displacement from the N_2P_2 least-squares plane (111.8 pm) than in **1b**. Thus, the conformation of the metallacycle in **2** is closer to that of neodymium complex **1c** than to that of starting material **1b**. Clearly, the different conformation of the six-membered metallacycle of **1b** compared to **1a**, **1c**, and **1d** is not only caused by the larger ionic radius of the lanthanum atom but also by the crystal packing. The distance between the central carbon atom C1 and the lanthanum atom (284.5(2) pm) is slightly longer than in **1b** (280.2(4) pm). The La–N bond lengths are in the expected ranges (La–N1 253.06(14), La–N2 251.22(15), La–N3 250.30(15), La–N4 243.29(15) pm). As a result of the asymmetric location of the $[(Ph_2P)_2N]^-$ ligand with respect to the $[CH(PPh_2NSiMe_3)_2]^-$ ligand, there is a small difference between the La–N1 and La–N2 bond lengths.

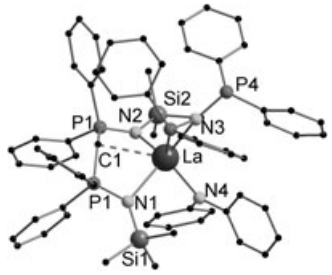

Figure 3. Solid-state structure of **2** showing the atom labeling scheme and omitting hydrogen atoms. Selected bond lengths [pm] and angles [°]: La–C1 284.5(2), La–N1 253.06(14), La–N2 251.22(15), La–N3 250.30(15), La–N4 243.29(15), La–P3 297.44(6), P1–C1 174.2(2), P2–C1 173.04(2), N1–P1 159.81(14), N2–P2 159.98(15), N3–P3 167.80(15), N3–P4 171.86(14); N4-La-N3 114.39(5), N4-La1-N2 102.51(5), N4-La–N1 90.76(5), N3-La–N2 115.88(5), N3-La–N1 123.83(5), N2-La1-N1 105.05(5).

Evidently, ligands of different steric demand can be attached to the metal center in high yields by using the right reaction order. Whereas the $[NPh_2]^-$ and the $[(Ph_2P)_2N]^-$ ligands can be coordinated several times onto a lanthanide atom, the $[CH(PPh_2NSiMe_3)_2]^-$ ligand could so far only be attached once to a trivalent lanthanide center. Thus, by attaching the $[CH(PPh_2NSiMe_3)_2]^-$ ligand in the first reaction step or by starting from $[\{(Ph_2P)_2N\}LnCl_2(thf)_3]$, a multiple coordination of the second largest ligand $[(Ph_2P)_2N]^-$ is not possible. In contrast, it was shown previously that two equivalents of the small $[NPh_2]^-$ ligand could fit around the metal center, and thus complexes of composition $[\{CH(PPh_2NSiMe_3)_2\}Ln(NPh_2)_2]$ (Ln = Y, Sm) were isolated.[9] To obtain all reaction products in high yields it is essential to attach the $[NPh_2]^-$ ligand in the last step. Thus, the whole reaction sequence shown in this paper is based on the steric demand of the ligands.

Polymerization catalysis: The efficiency of complexes **1a–d** and **2** as precatalysts for polymerization reactions was assayed with ε-caprolactone (CL) and methyl methacrylate (MMA). Complexes **1** and **2** showed high activity in polymerization of CL at room temperature (Table 1). Molar monomer/initiator ratios of 240–440/1 afforded polycaprolactone in good yields within a short time. The catalytic activity of **1a–d** depends on the ionic radius of the metal center. The lanthanum and neodymium compounds **1b** and **1c** gave high conversions within 5 min without any cocatalyst. Longer reaction times increased the yield only for **1b** and **1d**. After CL was added to the initiator solution, the reaction mixture becomes a solid gel within seconds. We believe the high viscosity of the reaction mixture prevents

Table 1. Polymerization of ε-caprolactone using **1a–d** and **2** as catalyst.[a]

Entry	Cat.	CL/Cat.[b]	Time [min]	Yield[c] [%]	M_n (calcd)[d] [g mol^{-1}]	M_n (exptl)[e] [g mol^{-1}]	D [g mol^{-1}]	M_n (corr)[f] [g mol^{-1}]	M_n (corr)/ M_n (calcd)
1	**1a**	388	5	5	2200	12700	1.75	7100	3.23
2	**1a**	289	120	94	30900	48700	2.1	27300	0.88
3	**1b**	423	5	100	48300	19600	3.58	11000	0.23
4	**1b**	330	120	94	35400	38000	1.97	21280	0.6
5	**2**	422	5	81	39000	31600	1.98	17700	0.45
6	**2**	338	120	84	32400	8900	2.48	5000	0.15
7	**1c**	307	5	81	28400	17600	4.4	9900	0.35
8	**1c**	238	120	93	25300	27200	1.87	15200	0.6
9	**1d**	436	5	12	6000	30200	1.77	16900	2.82
10	**1d**	294	120	58	19500	50000	2.29	28000	1.44

[a] Reaction conditions: room temperature, toluene. [b] Initial molar CL/catalyst ratio. [c] Determined gravimetrically. [d] Calculated from $M_{monomer}$·[M]/[I]·yield. [e] Measured by GPC. [f] Values obtained from GPC multiplied by 0.56.[25]

higher conversions. A comparison between the lanthanum compounds **1b** and **2** shows that complex **2** is slightly less active.

The resulting polycaprolactones have polydispersities between 1.8 and 4.4 regardless of the used initiator. For poor conversions (Table 1, entries 1, 9, and 10) the resulting molecular masses are up to three times higher than the theoretical values, whereas for high conversions M_n is significantly smaller. This deviation corresponds with particularly high polydispersities. Based on these results we suggest that one initiator molecule may successively start several polymer chains.

Polymerization of MMA was performed under a range of conditions (Table 2). The reactions were investigated at different temperatures with and without Me_3Al or Et_3Al as cocatalyst. All complexes are efficient catalysts, and the highest activity was found for **1b**. The activity and the selectivity are strongly dependent on the nature of the metal center. Furthermore, the activities are solvent-dependent; for example, yttrium complex **1a** does not show activity in toluene, but a moderate yield is obtained when THF is used as solvent (Table 2, entry 5). The obtained polymer shows a broad molecular mass distribution and rather high syndiotacticity. In contrast, the corresponding lanthanum compound **1b** is much more active. Polymerization starts without any cocatalyst, but small amounts of Et_3Al increase the yield significantly. Polymers produced without Et_3Al or at higher temperature were insoluble and chromatographically not acces-

Table 2. Polymerization of MMA with **1a–d** and **2** as catalyst.[a]

Entry	Cat.	Cocat.	Cat./Cocat./ MMA[b]	T [°C]	Time [h]	Yield[c] [%]	M_n (calcd)[d] [g mol^{-1}]	M_n (exptl)[e] [g mol^{-1}]	D	Tacticity[f] mm	mr	rr
1	**1a**	–	1/0/386	23	2	4	1500	n.d.[g]				
2	**1a**	–	1/0/372	−78	2	3	1100	n.d.				
3	**1a**	Me_3Al	1/6/304	23	2	1	300	n.d.				
4	**1a**	Me_3Al	1/7/346	−78	2	1	300	n.d.				
5[a]	**1a**	Me_3Al	1/9/401	−78	2	61	24500	35200	2.58	5	18	77
6	**1b**	–	1/0/420	25	2	4	1700	insoluble				
7	**1b**	Et_3Al	1/9/420	25	2	62	26100	insoluble				
8	**1b**	–	1/0/420	−78	2	27	11400	insoluble				
9	**1b**	Et_3Al	1/9/420	−78	2	96	40400	31200	1.32	4	20	76
10	**1b**	Et_3Al	1/8/940	−78	2	97	91100	63900	1.22	4	27	70
11	**1b**	Et_3Al	1/8/1900	−78	2	74	139000	99600	1.46	2	18	80
12	**2**	–	1/0/318	60	2	11	3500	n.d.				
13	**2**	–	1/0/318	23	2	29	9200	35000	2.15	21	47	32
14	**2**	–	1/0/287	−78	2	15	4300	3200	1.97			
15	**2**	Me_3Al	1/7/327	−78	2	78	25500	56900	1.84	3	33	64
16	**2**	Me_3Al	1/30/2866	−78	16	16	45900	63400	1.76	7	25	69
17	**1c**	–	1/0/426	50	1	0						
18	**1c**	–	1/0/266	25	1	0						
19	**1c**	–	1/0/426	78	1	0						
20	**1c**	Me_3Al	1/8/355	25	72	11	3900	60800	2.14	5	33	62
21	**1c**	Me_3Al	1/9/427	−78	2	33	14100	11000	1.31	9	29	62
22	**1c**	Et_3Al	1/9/428	−78	2	100	43100	27100	1.38	6	24	70
23	**1d**	–	1/0/349	23	2	9	3200	n.d.				
24	**1d**	–	1/0/401	−78	2	9	3600	n.d.				
25	**1d**	Me_3Al	1/6/271	23	2	63	17100	27000	1.54	4	35	61
26	**1d**	Me_3Al	1/6/271	−78	2	100	27100	26800	1.39	5	24	71

[a] In toluene, except entry 5 in THF. [b] Initial molar catalyst/cocatalyst/monomer ratio. [c] Determined gravimetrically. [d] Calculated from $M_{monomer}$·[M]/[I]·yield. [e] Measured by GPC. [f] Triad tacticity determined by ^{1}H NMR analysis. [g] Not determined because of too little polymeric product.

sible (Table 2, entries 6–8). Attempts to scale up the reaction by increasing the monomer/initiator ratio were successful (Table 2, entries 10 and 11). The molar monomer/initiator ratio was increased up to 1900/1 to afford the corresponding polymer with good yield (Table 2, entry 11). The MMA polymerization initiated by compound **1b** is sensitive to high temperature. The highest yields (almost quantitative) are obtained at reaction temperatures of −78 °C. The GPC analyses of the resulting basically syndiotactic polymers reveal narrow polydispersities and high molar masses. The latter are smaller than the calculated masses by factor of 0.7. The exchange of the chloro ligand for the $[NPh_2]^-$ ligand as a potential leaving group in compound **2** does not increase initiator activity. Alternatively, using compound **2** as the catalyst results in a larger fraction of atactic PMMA (Table 2, entry 13).

The activities of the neodymium and ytterbium complexes **1c** and **1d** are lower than those of the lanthanum compounds. Neither **1c** nor **1d** initiates MMA polymerization without the addition of a cocatalyst (Table 2, entries 17–19, 23, and 24). With **1c** as catalyst the polymer yield can be increased by decreasing the temperature, and it is even quantitative when Et_3Al is used instead of Me_3Al as cocatalyst (Table 2, entry 22). On addition of monomer the light blue color of the catalyst solution turns yellow and an exothermic reaction takes place. At low temperature the molecular mass of the polymer obtained is lower than expected and the polydispersity index and the tacticity are moderate, whereas at room temperature the obtained molecular masses exceed the calculated values enormously. In contrast, with **1d** as catalyst at low temperatures the obtained polymer shows a molar mass that corresponds well to the expected value (Table 2, entries 25 and 26) and a good tacticity is observed.

Conclusion

In summary, a series of lanthanide complexes having the bulky $[CH(PPh_2NSiMe_3)_2]^-$ and the flexible $[(Ph_2P)_2N]^-$ ligand in the same molecule were prepared by three different reaction pathways. The single-crystal X-ray structures of the resulting complexes $[\{CH(PPh_2NSiMe_3)_2\}Ln\{(Ph_2P)_2N\}Cl]$ (Ln = Y, La, Nd, Yb) show that the conformation of the six-membered metallacycle (N1-P1-C1-P2-N2-Ln) which is formed by chelation of the $[CH(PPh_2NSiMe_3)_2]^-$ ligand to the lanthanide atom is influenced by the ionic radius of the metal center. In solution dynamic behavior of the $[(Ph_2P)_2N]^-$ ligand is observed, which is caused by the rapid exchange of the two different phosphorus atoms. Further reaction of $[\{CH(PPh_2NSiMe_3)_2\}La\{(Ph_2P)_2N\}Cl]$ with $KNPh_2$ resulted in the heteroleptic amido complex $[\{(Me_3SiNPPh_2)_2CH\}La\{N(PPh_2)_2\}(NPh_2)]$. To isolate all reaction products in high yields it is necessary to attach the $[NPh_2]^-$ ligand in the last step. Thus, the whole reaction sequence shown here is based on the steric demand of the ligands. Both kinds of complexes, **1a–d** and **2**, are active for the ring-opening polymerization of ε-caprolactone and the polymerization of methyl methacrylate. In both cases the catalytic activity strongly depends on the ionic radius of the metal center. By using the lanthanum and neodymium compounds **1b** and **1c**, high conversions were achieved within a short time. The heteroleptic amido complex **2** shows in comparison to **1b** slightly lower activity. By using **1b** in MMA polymerization, high molecular weight polymers with good conversions and narrow polydispersities were obtained.

Experimental Section

General: All manipulations of air-sensitive materials were performed with the rigorous exclusion of oxygen and moisture in flame-dried Schlenk-type glassware on a dual-manifold Schlenk line, interfaced to a high-vacuum (10^{-4} Torr) line, or in an argon-filled M. Braun glove box. Ether solvents (THF and diethyl ether) were predried over Na wire and distilled under nitrogen from K (THF) or Na wire (ethyl ether) as well as benzophenone ketyl prior to use. Hydrocarbon solvents (toluene and *n*-pentane) were distilled under nitrogen from $LiAlH_4$. All solvents for vacuum-line manipulations were stored in vacuo over $LiAlH_4$ in resealable flasks. Deuterated solvents were obtained from Chemotrade Chemiehandelsgesellschaft mbH (all ≥ 99 atom % D) and were degassed, dried, and stored in vacuo over Na/K alloy in resealable flasks. NMR spectra were recorded on a Bruker AC 250 or JNM-LA 400 FT-NMR spectrometer. Chemical shifts are referenced to internal solvent resonances and are reported relative to tetramethylsilane (^1H, ^{13}C NMR) and 85 % phosphoric acid (^{31}P NMR). IR spectra were obtained on a Shimadzu FTIR-8400s. Elemental analyses were carried out with an Elementar vario EL. Polymer molecular masses and molecular mass distributions were measured by gel permeation chromatography (GPC) at 25 °C, a flow rate of 1.0 mL min^{-1}, and THF as eluent on a Waters 150 C instrument equipped with an interferometric refractometer (Wyatt, Optilab DSP). The PLgel Mixed-C column was calibrated against narrowly distributed PMMA standards or PS standards in the case of polycaprolactones. Chromatograms were processed with PSS WinGPC software. ^1H NMR spectra for analysis of the tacticity were recorded in $CDCl_3$ on a Bruker ARX 200. $LnCl_3$,[22] $K[CH(PPh_2NSiMe_3)_2]$,[15] $[\{[CH(PPh_2NSiMe_3)_2]LnCl_2\}_2]$,[9] $[\{(Ph_2P)_2N\}LnCl_2(thf)_3]$,[18] and $[K(THF)_nN(PPh_2)_2]$ ($n = 1.25$, 1.5)[14] were prepared according to literature procedures.

$[\{(Me_3SiNPPh_2)_2CH\}Ln\{N(PPh_2)_2\}Cl]$ (Ln = Y (1a), La (1b), Nd (1c), Yb (1d)): *Route A*: THF (20 mL) was condensed at −196 °C onto a mixture of $[\{[CH(PPh_2NSiMe_3)_2]LnCl_2\}_2]$ (0.25 mmol) and of $[K(thf)_nN(PPh_2)_2]$ (250 mg, 0.5 mmol) and the mixture was stirred for 18 h at room temperature. The solvent was then evaporated in vacuo and toluene (20 mL) was condensed onto the mixture. The mixture was filtered and the solvent was removed in vacuo. The product was recrystallized from hot toluene.

Route B: THF (20 mL) was condensed at −196 °C onto a mixture of $K[(Me_3SiNPPh_2)_2CH]$ (328 mg, 0.55 mmol) and $[\{(Ph_2P)_2N\}LnCl_2(thf)_3]$ (0.5 mmol) and the mixture was stirred for 18 h at room temperature. The solvent was then evaporated in vacuo and toluene was condensed onto the mixture. The mixture was briely refluxed and then filtered and the solvent was removed in vacuo. The product was crystallized from THF/*n*-pentane (1/2).

Route C: THF (20 mL) was condensed at −196 °C onto a mixture of $K[(Me_3SiNPPh_2)_2CH]$ (300 mg, 0.5 mmol), $LnCl_3$ (0.5 mmol), and $[K(thf)_nN(PPh_2)_2]$ (250 mg, 0.5 mmol). The mixture was stirred for 18 h at room temperature. The suspension was filtered and the solvent was removed in vacuo. The product was crystallized from THF/*n*-pentane (1/2) or hot toluene.

1a (Ln = Y, Routes A, B, and C): Yield 169 mg (32 %, Route A), colorless crystals. ^1H NMR ([D$_8$]THF, 250 MHz, 25 °C): $\delta = 0.00$ (s, 18H;

$SiMe_3$), 1.62–1.64 (m, 1H; CH), 6.94–7.61 ppm (m, 40H; Ph); $^{13}C\{^1H\}$ NMR ([D$_8$]THF, 62.9 MHz, 25°C): $\delta = 4.2$ ($SiMe_3$), 17.1 (t, CH, $^1J(C,P) = 93$ Hz), 128.0–129.1 (m, Ph), 131.2 (Ph), 131.9–134.1 (m, Ph), 135.1 (Ph), 136.6 (Ph), 142.8–143.0 ppm (m, Ph); ^{29}Si NMR ([D$_8$]THF, 49.7 MHz, 25°C): $\delta = -1.2$ ppm; $^{31}P\{^1H\}$ NMR ([D$_8$]THF, 101.3 MHz, 25°C): $\delta = 20.6$ (d, $^2J(P,Y) = 7.7$ Hz, PCP), 41.2 ppm (d, $^2J(P,Y) = 7.7$ Hz, PNP); elemental analysis calcd (%) for $C_{55}H_{59}ClN_3P_4Si_2Y$ (1066.47): C 61.94, H 5.58, N 3.94; found: C 61.65, H 5.66, N 3.78.

1b (Ln = La, Routes B and C): Yield 460 mg (78%, Route B), colorless crystals. ^1H NMR ([D$_8$]THF, 400 MHz, 25°C): $\delta = 0.01$ (s, 18H; $SiMe_3$), 1.74–1.79 (m, 4H; THF), 1.87–1.89 (m, 1H; CH), 3.58–3.63 (m, 4H; THF), 6.85–7.74 ppm (m, 40H; Ph); $^{29}Si\{^1H\}$ NMR ([D$_8$]THF, 79.3 MHz, 25°C): $\delta = -3.0$ ppm; $^{31}P\{^1H\}$ NMR ([D$_8$]THF, 161.7 MHz, 25°C): $\delta = 19.3$ (PCP), 41.3 ppm (PNP); IR (KBr): $\tilde{\nu} = 3051$ (m, ν(C=C*H*)), 2947 (m, ν(CH)), 1478 (w), 1435 (s), 1122 (m), 1095 (m), 923 (m), 917 (m), 897 (m), 833 (s), 739 (s), 693 cm^{-1} (vs); elemental analysis calcd (%) for $C_{59}H_{67}ClLaN_3OP_4Si_2$ (**1b**·THF, 1188.58): C 59.62, H 5.68, N 3.54; found: C 59.78, H 5.66, N 3.45.

1c (Ln = Nd, Route C): Yield 399 mg (66%, Route C), blue violet crystals. IR (KBr): $\tilde{\nu} = 3067$ (m, ν(C=C*H*)), 3050 (m, ν(C=C*H*)), 2947 (w, ν(CH)), 1478 (m), 1435 (s), 1247 (m), 1124 (s), 1095 (s), 1085 (s), 1061 (m), 912 (m), 897 (s), 835 (s), 739 (s), 706 (s), 693 cm^{-1} (s); elemental analysis calcd (%) for $C_{62}H_{67}ClN_3NdP_4Si_2$ (**1c**·toluene, 1213.94): C 61.34, H 5.56, N 3.46; found: C 60.97, H 5.44, N 3.29.

1d (Ln = Yb, Routes A and C): Yield 408 mg (71%, Route B), yellow-orange crystals. IR (KBr): $\tilde{\nu} = 3052$ (m, ν(C=C*H*)), 2947 (w, ν(CH)), 1478 (m), 1433 (s), 1148 (m), 1117 (s), 1088 (s), 1061 (m), 920 (m), 897 (s), 838 (s), 740 (s), 715 (s), 692 cm^{-1} (s); elemental analysis calcd (%) for $C_{55}H_{59}ClN_3P_4Si_2Yb$ (1150.60): C 57.41, H 5.17, N 3.65; found: C 57.59, H 5.23, N 3.35.

[{(Me$_3$SiNPPh$_2$)$_2$CH}La{N(PPh$_2$)$_2$}(NPh$_2$)] (2): Toluene (20 mL) was condensed at −196°C onto a mixture of **1b** (594 mg 0.5 mmol) and K[Ph$_2$N] (104 mg, 0.5 mmol) and the mixture was stirred for 18 h at room temperature. The mixture was filtered, and the solvent was removed in vacuo. The product was recrystallized from THF/*n*-pentane (1/2). Yield: 558 mg (89%), colorless crystalline rods. ^1H NMR ([D$_8$]THF, 400 MHz, 25°C): $\delta = -0.50$ (s, 18H; $SiMe_3$), 1.94 (t, 1H; CH, $^2J(H,P) = 5.1$ Hz), 6.61–6.67 (m, 2H; Ph), 6.95–7.45 (m, 44H; Ph), 7.60–7.67 ppm (m, 4H; Ph); $^{13}C\{^1H\}$ NMR ([D$_8$]THF, 100.4 MHz, 25°C): $\delta = 3.3$ ($SiMe_3$), 16.3 (t, CH, $^1J(C,P) = 110$ Hz), 118.5 (Ph), 120.8 (Ph), 128.4–129.0 (m, Ph), 130.5 (Ph), 131.3–133.7 (m, Ph), 143.9–144.2 (m, Ph), 154.3 ppm (Ph); $^{31}P\{^1H\}$ NMR ([D$_8$]THF, 161.7 MHz, 25°C): $\delta = 19.9$ (PCP), 43.1 ppm (PNP); elemental analysis calcd (%) for $C_{67}H_{69}LaN_4P_4Si_2$ (1249.23): calcd: C 64.42, H 5.57, N 4.48; found: C 64.28, H 5.49, N 4.33.

Polymerization experiments: All polymerization experiments were carried out by standard Schlenk techniques under a nitrogen atmosphere. Methyl methacrylate (MMA) and ε-caprolactone (CL) were dried over CaH_2 and distilled prior to use. In a typical procedure a Schlenk flask was charged with 30 mg of catalyst complex. The complex was dissolved in dry toluene (5 mL) and mixed with 1 mL of a 0.2 M solution of $AlEt_3$ in toluene, and 1 mL of monomer was added by syringe. After 2 h the polymerization was quenched by adding 5 mL of acidified methanol. The quenched mixture was precipitated into 100 mL of methanol, stirred, filtered, washed with methanol, and dried at room temperature at 10^{-2} mbar.

X-ray crystallographic studies on 1a–d and 2: Crystals of **1a–d** were grown from THF/*n*-pentane (1/2) or from hot toluene. Crystals of **2** were obtained from THF/*n*-pentane (1/2). A suitable crystal was covered in mineral oil (Aldrich) and mounted onto a glass fiber. The crystal was transferred directly to the −73°C or −100°C N_2 cold stream of a Stoe IPDS II or a Brucker Smart 1000 CCD diffractometer. Subsequent computations were carried out on an Intel Pentium III PC.

All structures were solved by the Patterson method (SHELXS-97[23]). The remaining non-hydrogen atoms were located from successive difference Fourier map calculations. The refinements were carried out by using full-matrix least-squares techniques on *F*, minimizing the function $(F_o - F_c)^2$, where the weight is defined as $4F_o^2/2(F_o^2)$ and F_o and F_c are the observed and calculated structure factor amplitudes, using the program SHELXL-97.[24] Carbon-bound hydrogen atom positions were calculated and allowed to ride on the carbon atom to which they are bonded by assuming a C–H bond length of 0.95 Å. The hydrogen atom contributions were calculated but not refined. The locations of the largest peaks in the final difference Fourier map and the magnitude of the residual electron densities in each case were of no chemical significance. Positional parameters, hydrogen atom parameters, thermal parameters, bond lengths and angles have been deposited as Supporting Information. CCDC-251953–CCDC-251957 contain the supplementary crystallographic data for this paper. These data can be obtained free of charge from The Cambridge Crystallographic Data Centre via www.ccdc.cam.ac.uk/data_request/cif.

1a: $C_{55}H_{59}ClN_3P_4Si_2Y$, triclinic, $P\bar{1}$ (no. 2); $a = 1009.6(8)$, $b = 1351.6(11)$, $c = 2123.8(15)$ pm, $\alpha = 90.47(6)$, $\beta = 101.10(6)$, $\gamma = 109.63(5)°$; $V = 2670(4) \times 10^6$ pm^3, $Z = 2$; $\mu(Mo_{K\alpha}) = 1.346$ mm^{-1}; $\theta_{max} = 25°$; 8844 ($R_{int} = 0.0453$) independent reflections measured, of which 6494 were considered observed with $I > 2\sigma(I)$; max./min. residual electron density 0.584/−0.990 e A^{-3}; 601 parameters, $R1 = 0.0457$ ($I > 2\sigma(I)$); w$R2 = 0.1121$ (all data).

1b·THF: $C_{59}H_{67}ClLaN_3OP_4Si_2$, monoclinic, $P2_1/n$ (no. 14); $a = 1060.0(2)$, $b = 2772.9(6)$, $c = 2057.1(4)$ pm, $\beta = 99.66(3)°$; $V = 5960(2) \times 10^6$ pm^3, $Z = 4$; $\mu(Mo_{K\alpha}) = 0.950$ mm^{-1}; $\theta_{max} = 30.58$; 18281 ($R_{int} = 0.0625$) independent reflections measured, of which 13734 were considered observed with $I > 2\sigma(I)$; max./min. residual electron density 4.644/−1.476 e A^{-3}; 621 parameters, $R1 = 0.0702$ ($I > 2\sigma(I)$); w$R2 = 0.1815$ (all data).

1c·toluene: $C_{62}H_{67}ClN_3NdP_4Si_2$, triclinic, $P\bar{1}$ (no. 2); $a = 1189.90(2)$, $b = 1310.1(2)$, $c = 1973.4(3)$ pm, $\alpha = 79.567(3)$, $\beta = 83.876(3)$, $\gamma = 89.249(3)°$; $V = 3008.0(7) \times 10^6$ pm^3, $Z = 2$; $\mu(Mo_{K\alpha}) = 1.094$ mm^{-1}; $\theta_{max} = 30.58$; 18170 ($R_{int} = 0.0463$) independent reflections measured, of which 11558 were considered observed with $I > 2\sigma(I)$; max./min. residual electron density 1.920/−1.031 e A^{-3}; 470 parameters, $R1 = 0.0526$ ($I > 2\sigma(I)$); w$R2 = 0.1319$ (all data).

1d: $C_{55}H_{59}ClN_3P_4Si_2Yb$, triclinic, $P\bar{1}$ (no. 2); $a = 1007.5(4)$, $b = 1346.1(7)$, $c = 2123.4(7)$ pm, $\alpha = 90.07(3)$, $\beta = 100.82(3)$, $\gamma = 109.44(3)°$; $V = 2661(2) \times 10^6$ pm^3, $Z = 2$; $\mu(Mo_{K\alpha}) = 2.012$ mm^{-1}; $\theta_{max} = 25.00$; 8801 ($R_{int} = 0.0461$) independent reflections measured, of which 8105 were considered observed with $I > 2\sigma(I)$; max./min. residual electron density 1.888 and −2.581 e A^{-3}; 601 parameters, $R1 = 0.0445$ ($I > 2\sigma(I)$); w$R2 = 0.1219$ (all data).

2: $C_{67}H_{69}LaN_4P_4Si_2$, monoclinic, $P2_1/n$ (no. 14); $a = 1358.8(2)$, $b = 2266.8(4)$, $c = 2124.5(4)$ pm, $\beta = 106.590(4)°$; $V = 6271(2)$ 10^6 pm^3, $Z = 4$; $\mu(Mo_{K\alpha}) = 0.864$ mm^{-1}; $\theta_{max} = 33.42$; 22772 ($R_{int} = 0.0315$) independent reflections measured, of which 16795 were considered observed with $I > 2\sigma(I)$; max./min. residual electron density 2.934/−0.613 e A^{-3}; 709 parameters, $R1 = 0.0326$ ($I > 2\sigma(I)$); w$R2 = 0.0827$ (all data).

Acknowledgements

This work was supported by the Deutsche Forschungsgemeinschaft and the Fonds der Chemischen Industrie. Additionally, generous support from Prof. Dr. D. Fenske is gratefully acknowledged.

[1] S. Kobayashi in *Lanthanides: Chemistry and Use in Organic Chemistry*, Springer, Heidelberg, **1999**, p. 256–283.

[2] a) H. Yasuda, H. Yamamoto, K. Yokota, S. Miyake, A. Nakamura, *J. Am. Chem. Soc.* **1992**, *114*, 4908–4910; b) H. Yasuda, H. Yamamoto, M. Yamashita, K. Yokota, A. Nakamura, S. Miyake, Y. Kai, N. Kanehisa, *Macromolecules* **1993**, *26*, 7134–7143.

[3] a) L. S. Boffa, B. M. Novak, *Macromolecules* **1994**, *27*, 6993–6995; b) E. Ihara, M. Morimoto, H. Yasuda, *Macromolecules* **1995**, *28*, 7886–7892.

[4] a) S. Y. Knjazhanski, L. Elizalde, G. Cadenas, B. M. Bulychev, *J. Organomet. Chem.* **1998**, *568*, 33–40; b) E. Ihara, K. Koyama, H. Yasuda, N. Kanehisa, Y. Kai, *J. Organomet. Chem.* **1999**, *574*, 40–49; c) G. Desurmont, Y. Li, H. Yasuda, T. Maruo, N. Kanehisa, Y. Kai, *Organometallics* **2000**, *19*, 1811–1813; d) G. Desurmont, T. To-

kimitsu, H. Yasuda, *Macromolecules* **2000**, *33*, 7679–7681; e) M. Glanz, S. Dechert, H. Schumann, D. Wolff, J. Springer, *Z. Anorg. Allg. Chem.* **2000**, *626*, 2467–2477; f) H. Schumann, M. Glanz, J. Gottfriedsen, S. Dechert, D. Wolff, *Pure Appl. Chem.* **2001**, *73*, 279–282; g) T. J. Woodman, M. Schormann, M. Bochmann, *Organometallics* **2003**, *22*, 2938–2943; h) C. Cui, A. Shafir, C. L. Reeder, J. Arnold, *Organometallics* **2003**, *22*, 3357–3359.

[5] a) M. Yamashita, Y. Takemoto, E. Ihara, H. Yasuda, *Macromolecules* **1996**, *29*, 1798–1806; b) K. C. Hultzsch, T. P. Spaniol, J. Okuda, *Organometallics* **1997**, *16*, 4845–4856; c) T. J. Woodman, M. Schormann, D. L. Hughes, M. Bochmann, *Organometallics* **2004**, *23*, 2972–2979; d) I. Palard, A. Soum, S. M. Guillaume, *Chem. Eur. J.* **2004**, *10*, 4054–4062.

[6] a) S. J. McLain, N. E. Drysdale, *Polym. Prepr.* **1992**, *33*, 174–175; b) W. M. Stevels, M. J. K. Ankone, P. J. Dijkstra, J. Feijen, *Macromolecules* **1996**, *29*, 3332–3333; c) Y. Shen, Z. Shen, Y. Zhang, K. Yao, Kemin, *Macromolecules* **1996**, *29*, 8289–8295; d) K. Tortosa, T. Hamaide, C. Boisson, R. Spitz, *Macromol. Chem. Phys.* **2001**, *202*, 1156–1160.

[7] a) T. G. Wetzel, S. Dehnen, P. W. Roesky, *Angew. Chem.* **1999**, *111*, 1155–1158; *Angew. Chem. Int. Ed.* **1999**, *38*, 1086–1088; b) S. Wingerter, M. Pfeiffer, F. Baier, T. Stey, D. Stalke, *Z. Anorg. Allg. Chem.* **2000**, *626*, 1121–1130.

[8] a) S. Anfang, K. Harms, F. Weller, O. Borgmeier, H. Lueken, H. Schilder, K. Dehnicke, *Z. Anorg. Allg. Chem.* **1998**, *624*, 159–166; b) S. Anfang, T. Gröb, K. Harms, G. Seybert, W. Massa, A. Greiner, K. Dehnicke, *Z. Anorg. Allg. Chem.* **1999**, *625*, 1853–1859; c) T. Gröb, G. Seybert, W. Massa, F. Weller, R. Palaniswami, A. Greiner, K. Dehnicke, *Angew. Chem.* **2000**, *112*, 4542–4544; *Angew. Chem. Int. Ed.* **2000**, *39*, 4373–4375; d) T. Gröb, G. Seybert, W. Massa, K. Dehnicke, *Z. Anorg. Allg. Chem.* **2001**, *627*, 304–306.

[9] M. T. Gamer, S. Dehnen, P. W. Roesky, *Organometallics* **2001**, *20*, 4230–4236.

[10] M. T. Gamer, P. W. Roesky, *J. Organomet. Chem.* **2002**, *647*, 123–127.

[11] K. Aparna, M. Furguson, R. G. Cavell, *J. Am. Chem. Soc.* **2000**, *122*, 726–727.

[12] a) F. T. Edelmann, *Top. Curr. Chem.* **1996**, *179*, 113–148; b) U. Reissmann, P. Poremba, M. Noltemeyer, H.-G. Schmidt, F. T. Edelmann, *Inorg. Chim. Acta* **2000**, *303*, 156–162; c) A. Recknagel, A. Steiner, M. Noltemeyer, S. Brooker, D. Stalke, F. T. Edelmann, *J. Organomet. Chem.* **1991**, *414*, 327–335; d) A. Recknagel, M. Witt, F. T. Edelmann, *J. Organomet. Chem.* **1989**, *371*, C40–C44.

[13] a) S. Agarwal, C. Mast, K. Dehnicke, A. Greiner, *Macromol. Rapid Commun.* **2000**, *21*, 195–212; b) P. Ravi, T. Groeb, K. Dehnicke, A. Greiner, *Macromolecules* **2001**, *34*, 8649–8653.

[14] P. W. Roesky, M. T. Gamer, M. Puchner, A. Greiner, *Chem. Eur. J.* **2002**, *8*, 5265–5271.

[15] M. T. Gamer, P. W. Roesky, *Z. Anorg. Allg. Chem.* **2001**, *627*, 877–881.

[16] a) A. Zulys, T. K. Panda, M. T. Gamer, P. W. Roesky, *Chem. Commun.* **2004**, 2584–2585; b) A. Zulys, T. K. Panda, M. T. Gamer, P. W. Roesky, *Organometallics* **2005**, *24*, in press.

[17] The bonding situation in the drawings of the ligand system in Schemes 1 and 2 is simplified for clarity.

[18] P. W. Roesky, M. T. Gamer, N. Marinos, *Chem. Eur. J.* **2004**, *10*, 3537–3542.

[19] F. T. Edelmann, D. M. M. Freckmann, H. Schumann, *Chem. Rev.* **2002**, *102*, 1851–1896.

[20] a) P. Imhoff, J. H. Guelpen, K. Vrieze, W. J. J. Smeets, A. L. Spek, C. J. Elsevier, *Inorg. Chim. Acta* **1995**, *235*, 77–88; b) C. M. Ong, P. McKarns, D. W. Stephan, *Organometallics* **1999**, *18*, 4197–4208; c) A. Kasani, R. P. Kamalesh Babu, R. McDonald, R. G. Cavell, *Organometallics* **1999**, *18*, 3775–3777; d) K. Aparna, R. McDonald, M. Fuerguson, R. G. Cavell, *Organometallics* **1999**, *18*, 4241–4243; e) P. Wei, D. W. Stephan, *Organometallics* **2002**, *21*, 1308–1310; f) M. J. Sarsfield, H. Steele, M. Helliwell, S. J. Teat, *Dalton Trans.* **2003**, 3443–3449; g) M. S. Hill, P. B. Hitchcock, *Dalton Trans.* 2003, 4570–4571; h) C. Bibal, M. Pink, Y. D. Smurnyy, J. Tomaszewski, K. G. Caulton, *J. Am. Chem. Soc.* **2004**, *126*, 2312–2313.

[21] M. T. Gamer, P. W. Roesky, *Inorg. Chem.* **2004**, *43*, 4903–4906.

[22] M. D. Taylor, C. P. Carter, *J. Inorg. Nucl. Chem.* **1962**, *24*, 387–391.

[23] G. M. Sheldrick, SHELXS-97, Program of Crystal Structure Solution, University of Göttingen, Germany, **1997**.

[24] G. M. Sheldrick, SHELXL-97, Program of Crystal Structure Refinement, University of Göttingen, Germany, **1997**.

[25] M. Save, M. Schappacher, A. Soum, *Macromol. Chem. Phys.* **2002**, *203*, 889–899.

Received: October 19, 2004
Published online: March 18, 2005